

Review Article

Rolled-Up Metamaterials

Stephan Schwaiger, Andreas Rottler, and Stefan Mendach

Institut für Angewandte Physik und Zentrum für Mikrostrukturforschung, Universität Hamburg, Jungiusstrasse 11, 20355 Hamburg, Germany

Correspondence should be addressed to Stefan Mendach, smendach@physnet.uni-hamburg.de

Received 18 August 2012; Accepted 25 September 2012

Academic Editor: Ivan D. Rukhlenko

Copyright © 2012 Stephan Schwaiger et al. This is an open access article distributed under the Creative Commons Attribution License, which permits unrestricted use, distribution, and reproduction in any medium, provided the original work is properly cited.

In this paper we review metamaterials fabricated from self-rolling strained metal-semiconductor layer systems. These systems relax their strain upon release from the substrate by rolling up into microtubes with a cross-section similar to a rolled-up carpet. We show that the walls of these microtubes represent three-dimensional optical metamaterials which so far could be used, for example, for the realization of broadband hyperlenses, fishnet metamaterials, or optically active three-dimensional metamaterials utilizing the unique possibility to stack optically active semiconductor heterostructures and metallic nanostructures. Furthermore, we discuss THz metamaterials based on arrays of rolled-up metal semiconductor microtubes and helices.

1. Introduction

While the concept of metamaterials, that is, tailoring the optical properties of a material to desired values by cleverly designing its subwavelength composites, is in principle scalable in frequency, the realization of three-dimensional metamaterials for optical frequencies remains one of the current challenges in the research area of metamaterials [1, 2]. Compared to the fabrication used in the pioneering works on metamaterials operating in the microwave regime [3–6], which were composed of millimeter-sized metallic structures produced with well-established printed circuit board techniques, the deliberate structuring on the nanoscale in three dimensions for the production of three-dimensional optical metamaterials is much more elaborate. Possible routes are, for example, stacking of single-layered metamaterials by repeating planar lithographic processing steps [7], focused ion beam milling of multilayers [8], multilayer deposition on patterned substrates [9, 10], galvanization in combination with three-dimensional laser interference lithography [11], or galvanization in combination with anodic oxidation [12]. Here we discuss three-dimensional metamaterials prepared by rolling up a single-layered metamaterial with multiple rotations into a radial stack, similar to rolling up a bilayer of biscuit and cream into a Swiss-roll cake. One possibility

to follow this route is actively rolling up the layer system as demonstrated by Gibbons and colleagues, who rolled up a gold-polymer bilayer around a millimeter-sized glass rod and obtained a high quality radial multilayer system [13]. Another possibility is utilizing the concept of strain induced self-rolling of nanolayers which was pioneered by Prinz and coworkers for the InGaAlAs semiconductor system [14, 15] and since then adopted to various kinds of material systems including metals, semiconductors, isolators, and hybrids thereof [16–22]. Smith and coworkers pointed out in theoretical works that rolled-up metal-isolator systems might be promising candidates for the realization of metamaterial waveguides [23] and hyperlenses [24, 25]. Particularly interesting are hybrid systems of semiconductors and metals, since they open up the unique possibility to stack electrically or optically active semiconductor layers and metallic components in order to obtain active metamaterials. In the following we review our work in this direction utilizing self-rolling strained InGaAlAs/metal layers for the realization of three-dimensional optical metamaterials including hyperlenses [26–28], fishnet metamaterials [29], and optically active metamaterials [30–32]. In addition we discuss the possibility to use arrays of rolled-up InGaAs/metal structures to realize metamaterials for far infrared frequencies [33, 34].

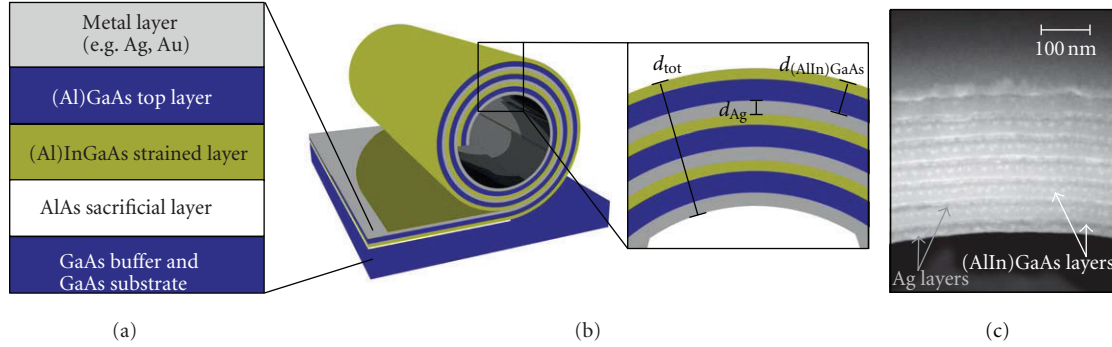


FIGURE 1: (a) layer sequence for producing a rolled-up metamaterial, (b) rolled-up multilayer of silver and (In)GaAs. Inset: the wall of the resulting tube represents a three-dimensional metamaterial. (c) Scanning electron microscopic cross-section image of a realized metamaterial consisting of 6 lattice cells with $d_{Ag} = 22$ nm and $d_{In} = 34$ nm.

2. Preparation of Rolled-Up Metamaterials

Figure 1(a) shows a typical layer sequence, as used, for example, for the preparation of the rolled-up hyperlens shown in Figure 1(c) and discussed in Section 3. Molecular beam epitaxy (MBE) is used to grow a typically 40 nm thick AlAs sacrificial layer followed by a strained (Al)InGaAs layer and an (Al)GaAs layer, each a few nanometers thick, on top of a GaAs substrate. On top of this strained semiconductor heterostructure a few nanometers thick metal film is deposited by thermal evaporation. After the selective etching of the AlAs sacrificial layer with buffered hydrofluoric acid, the strained layer system is detached from the substrate and rolls up into a tube as sketched in Figure 1(b). The walls of these tubes are the basic structure used for the optical three-dimensional metal-semiconductor metamaterials discussed in the following. Due to the fact that the entire structure comes from the same layer, rolled-up metamaterials exhibit a perfect uniformity and give the unique opportunity to stack identical MBE-grown semiconductor heterostructures with metallic structures. The tube diameter of the devices discussed here typically amounts to a few microns and can be controlled by the layer thicknesses and composition; the number of revolutions N is adjustable by the etching time. The passive rolled-up hyperlens structure consisting of nonfunctionalized semiconductor layers and planar metal films, as shown in Figure 1, is discussed in Section 3. Patterning the rolled-up structures shown in Figure 1 after the rolling-up process results in fishnet metamaterials as discussed in Section 4. In Sections 5 and 6 we demonstrate that quantum wells can be integrated into the semiconductor component of the rolled-up structures to realize optically active metamaterials. Optionally, the metal films can be replaced by plasmonic nanostructures, which are prepared onto the strained semiconductor prior to rolling up, as demonstrated in Section 6. A different ansatz using the same preparation technique but considering the whole tube as one cell of a metamaterial for the THz regime is addressed in Section 7.

3. Rolled-Up Hyperlens

Multistacks of thin metal layers and thin dielectric layers might be approximated as an effective medium with an anisotropic permittivity tensor as described, for example, in [35]. This permittivity tensor has on the major axis $\epsilon_{||} = (\epsilon_M + \eta\epsilon_D)/(1 + \eta)$ for the two directions in the plane of the layers and $\epsilon_{\perp} = (1 + \eta)/(1/\epsilon_M + \eta/\epsilon_D)$ for the direction perpendicular to the layers and zeros otherwise. In this case, ϵ_D is the permittivity of the dielectric layer, ϵ_M is the permittivity of the metal layer, and η is the layer thickness ratio of dielectric and metal layer. Due to the special ellipsoidal and hyperbolic shapes of their Fresnel surfaces, that is, their isofrequency surfaces in k space, one can use such media for subwavelength imaging under certain conditions [35–37]. For $0 < \epsilon_{||} \ll |\epsilon_{\perp}|$ one obtains flat extended iso-frequency surfaces in k space, which leads to the propagation of very high k components with a common group velocity perpendicular to the multilayers. This directed imaging of very fine details is called hyperlensing and, when using curved instead of flat multilayers, can be used to magnify subwavelength details with a magnification given by the ratio of outer and inner radius of the multilayer structure [38]. Cylindrical hyperlenses working in the ultraviolet [10] as well as spherical hyperlenses operating in the blue [9] could be realized in the group of Xiang Zhang by sequential deposition of layers of silver and dielectric on patterned substrates.

Rolled-up metamaterials made of silver-InGaAs multilayers are promising candidates for hyperlensing at near infrared and visible frequencies. Due to the significantly higher permittivity of the semiconductor compared to dielectrics like, for example, Aluminum Oxide or Titanium Oxide, the operation range, where the condition $0 < \epsilon_{||} \ll |\epsilon_{\perp}|$ is satisfied in silver-InGaAs multilayers, can easily be shifted over the visible and near infrared regime by choosing the respective layer ratio η . Experimentally, the zero crossing of $\epsilon_{||}$ and thus the lower cutoff frequency for hyperlensing operation can be obtained from transmission and reflection measurements. At normal incidence one expects $\epsilon_{||} < 0$ for

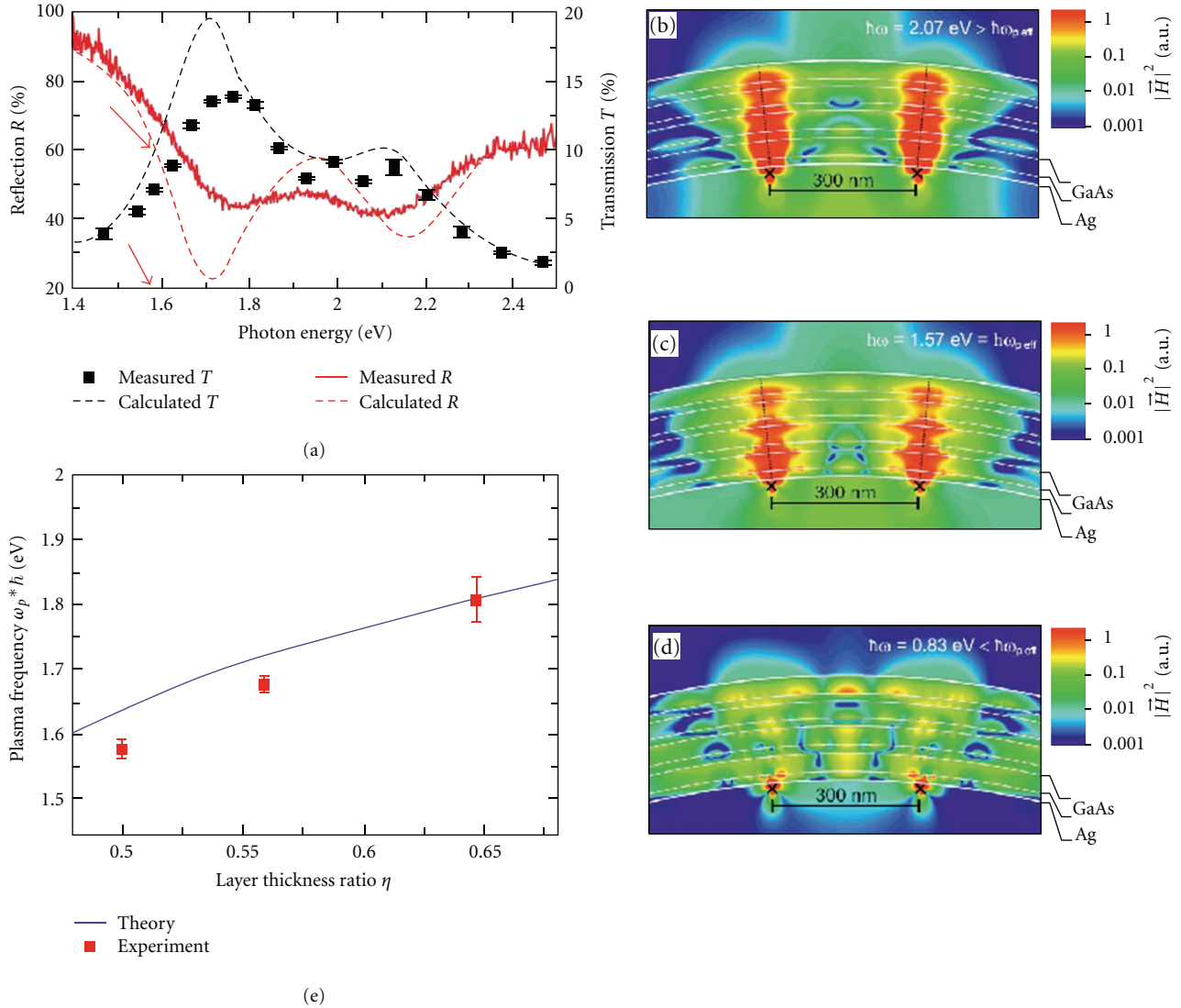


FIGURE 2: (a) Experimental reflectance and transmittance of a rolled-up hyperlens together with corresponding theoretical curves from transfer matrix calculations. (b), (c) Simulation of the imaging of two dipoles from the inside of the hyperlens to the outer perimeter for two frequencies above the plasma edge, (d) Corresponding simulation for a frequency below the plasma edge. (e) Experimentally observed frequency of the plasma edge as a function of layer thickness ratio of silver and InGaAs.

metallic reflection and $\epsilon_{||} > 0$ for dielectric transmission; that is, $\epsilon_{||} = 0$ marks the plasma edge of the effective material.

While the measurement of reflection from a rolled-up metamaterial can be performed with slight modifications of conventional reflection setups, the measurement of transmission through the rolled-up metamaterials is challenging since it requires a transmission light source inside the rolled-up structure. As sketched in Figure 4(a) in Section 5 we realize such a transmission source with a metal coated fiber which we manipulate into the rolled-up metamaterial by means of piezo actuators. Light scattered from a nanohole with typically a few 100 nm diameter, which is prepared into the metallization of the fiber tip by focused ion beams, is transmitted through the rolled-up metamaterial and collected with a microscope objective. As a reference

we measure the emission from the nanohole with the fiber tip outside of the rolled-up metamaterial. Figure 2(a) shows transmission measurements (black squares) and reflection measurements (red curve) of a rolled-up silver-InGaAs hyperlens ($\eta = 0.5$, $d_{Ag} = 17 \text{ nm}$, $d_{InGaAs} = 34 \text{ nm}$, $N = 4$), together with corresponding transfer matrix calculations. The red arrows indicate the plasma edge. At frequencies above the plasma edge distinct resonances appear. In [28] we could show that these resonances are due to Fabry-Perot interferences corresponding to the total layer thickness and can be used to enhance the transmission through a rolled-up hyperlens at desired frequencies. Towards high frequencies, the transmission decreases again due to the high absorption in the semiconductor component. As Figure 2(e) illustrates, we have experimentally demonstrated that the plasma edge

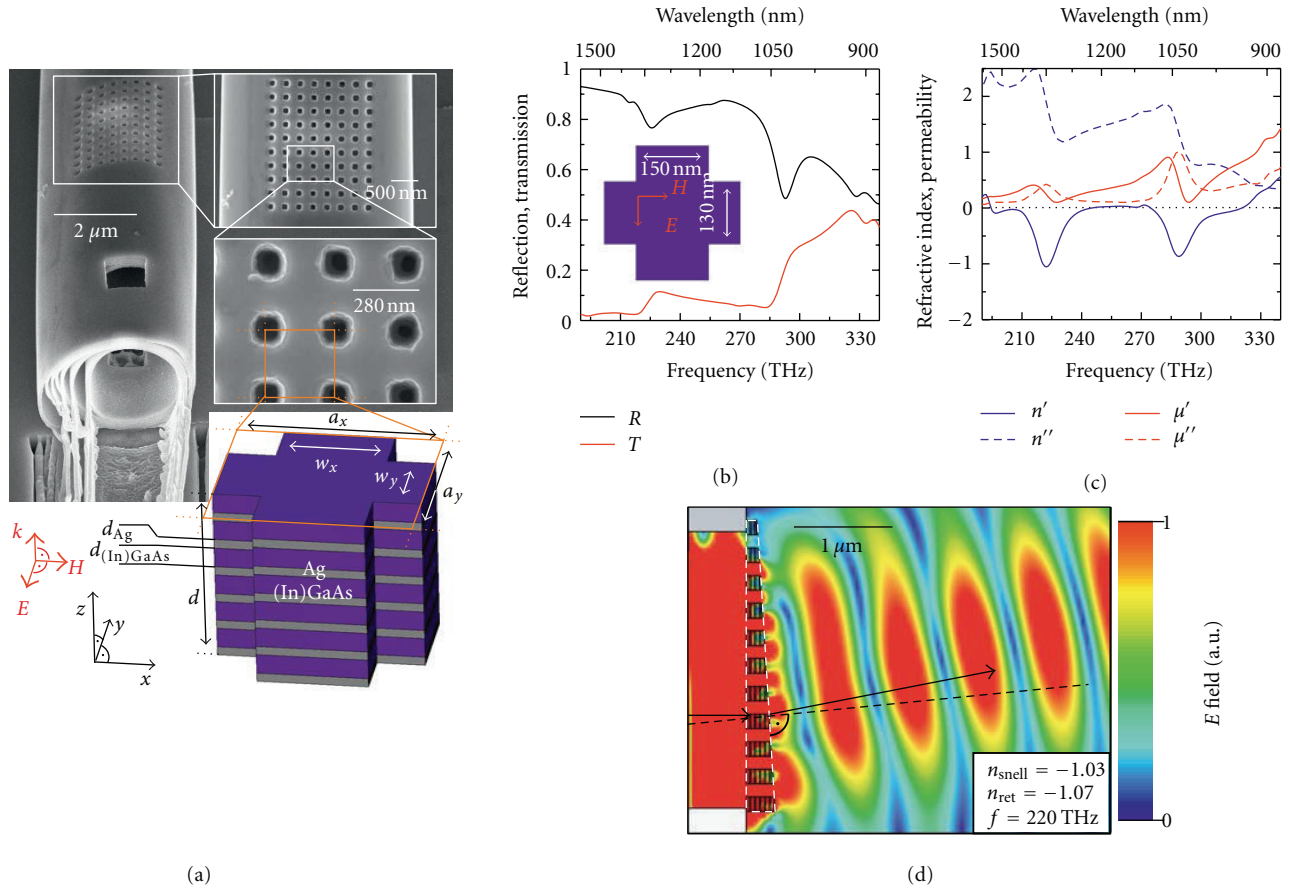


FIGURE 3: (a) Microroll with six alternating layers of metal and semiconductor with a fishnet pattern obtained by focused ion beam milling. As visible, the end of the tube exhibits noncompact layer stacking. Nevertheless, in the area of the fishnet pattern the layer stacking is compact. The sketch shows the unit cell of the fishnet pattern. The electromagnetic wave is incident in z direction. (b) Calculated reflection and transmission through the structure in (a). (c) The permeability ($\mu = \mu' + i\mu''$) and refractive index ($n = n' + in''$), calculated by a parameter retrieval method, reveal that n' becomes negative at certain frequencies. (d) A wave impinging from the left ($f = 220$ THz) gets negatively refracted by a prism that is cut into the fishnet structure. The prism is depicted by the white, dashed lines, with the structure infinitely extended in the direction perpendicular to the image plane. Figure reprinted from [29] with slight modifications.

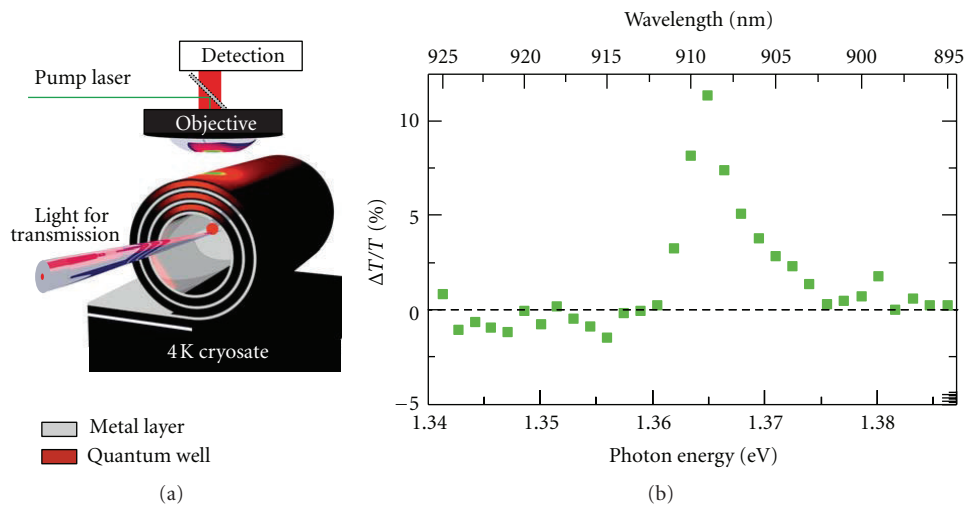


FIGURE 4: (a) Sketch of the setup for measurements of the transmission through an active rolled-up metamaterial. The setup allows to optically excite active layers, for example, InGaAs quantum wells, inside the metamaterial to enhance the light transmission. (b) The transmission enhancement of an active rolled-up metamaterial is plotted against the photon energy showing a pronounced maximum of $\Delta T/T = 10\%$ at a photon energy of $E = 1.36$ eV. Images taken from [30].

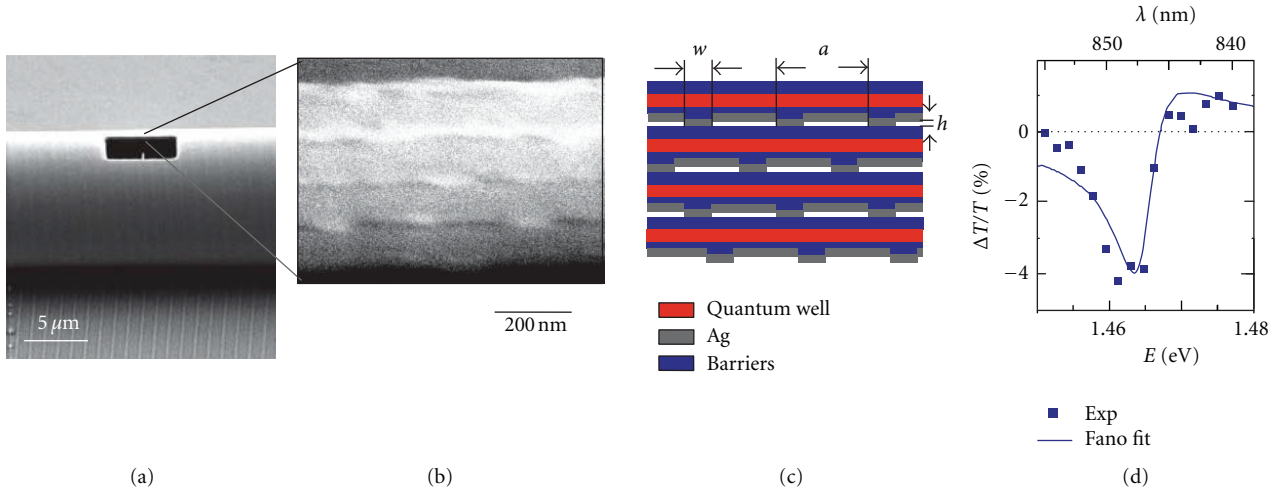


FIGURE 5: (a)-(b) Scanning electron micrographs of a rolled-up metamaterial consisting of a three-dimensional silver lattice interleaved with quantum wells. (c) Schematic of the metamaterial according to the cross-section shown in (b). (d) Pump-induced change in transmission through the metamaterial (blue squares), together with a Fano fit (blue line).

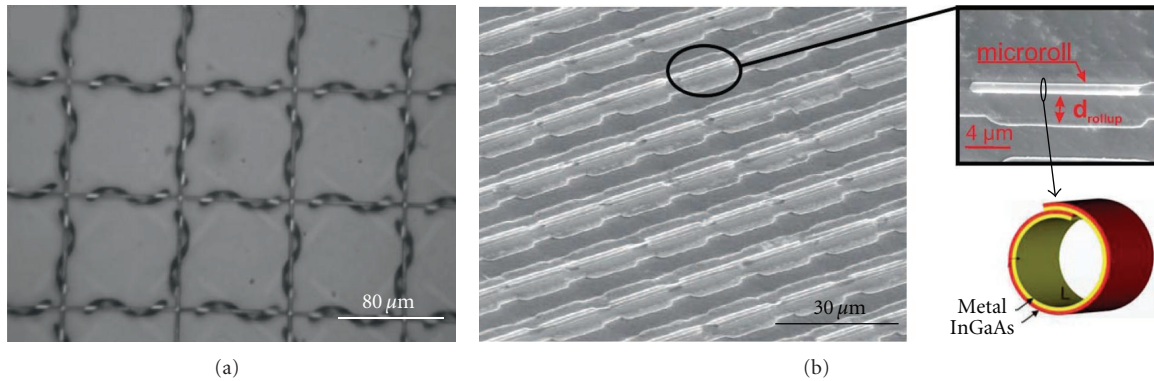


FIGURE 6: (a) Chiral metamaterial made of an array of rolled-up InGaAs/GaAs/Ti/Au microhelices realized by Prinz and coworkers. The material exhibits circular dichroism and linear polarization rotation in the operation frequency range around 2 THz. The image is taken from [34]. (b) Metamaterial made of an array of rolled-up InGaAs/GaAs/Cr microtubes. The zoom-in shows a single microtube. As sketched in the bottom right, the microtubes exhibit slightly more than one rotation resembling the concept of a split ring resonator [3]. We showed by means of finite difference time domain simulations that these structures might be used to obtain a magnetic response at THz frequencies.

can be shifted over the visible and near infrared regime by changing the layer thickness ratio η . Figures 2(b)–2(d) show finite difference time domain simulations (Lumerical FDTD Solutions) for light propagation in the hyperlens with a plasma edge at 1.57 eV (cf. Figure 2(a)). On the inner surface of the hyperlens two dipoles are placed at a distance of 300 nm. In fact, for frequencies at and above the plasma edge we observe hyperlensing, that is, radially directed imaging of the dipoles onto the outer hyperlens surface (Figures 2(b) and 2(c)). In contrast to this, no hyperlensing occurs for frequencies below the plasma edge (Figure 2(d)). A particularly interesting aspect of these simulations is the fact that hyperlensing occurs also for relatively thick individual layers as used in our structures, which exceed the individual layer thickness limit of approximately 5 nm for the

applicability of effective medium retrieval methods to our structures [27].

4. Three-Dimensional Fishnet Metamaterial with Negative Refractive Index at 1000 nm Wavelength

Figure 3(a) shows a rolled-up metamaterial similar to the one presented in Figure 1 with six windings, where an array of holes with diameters smaller than 100 nm has been cut into its wall using focused ion beam milling after the rolling-up process. In [29] we showed by means of finite difference time domain simulation that a negative index of refraction in the near-infrared regime is expected in

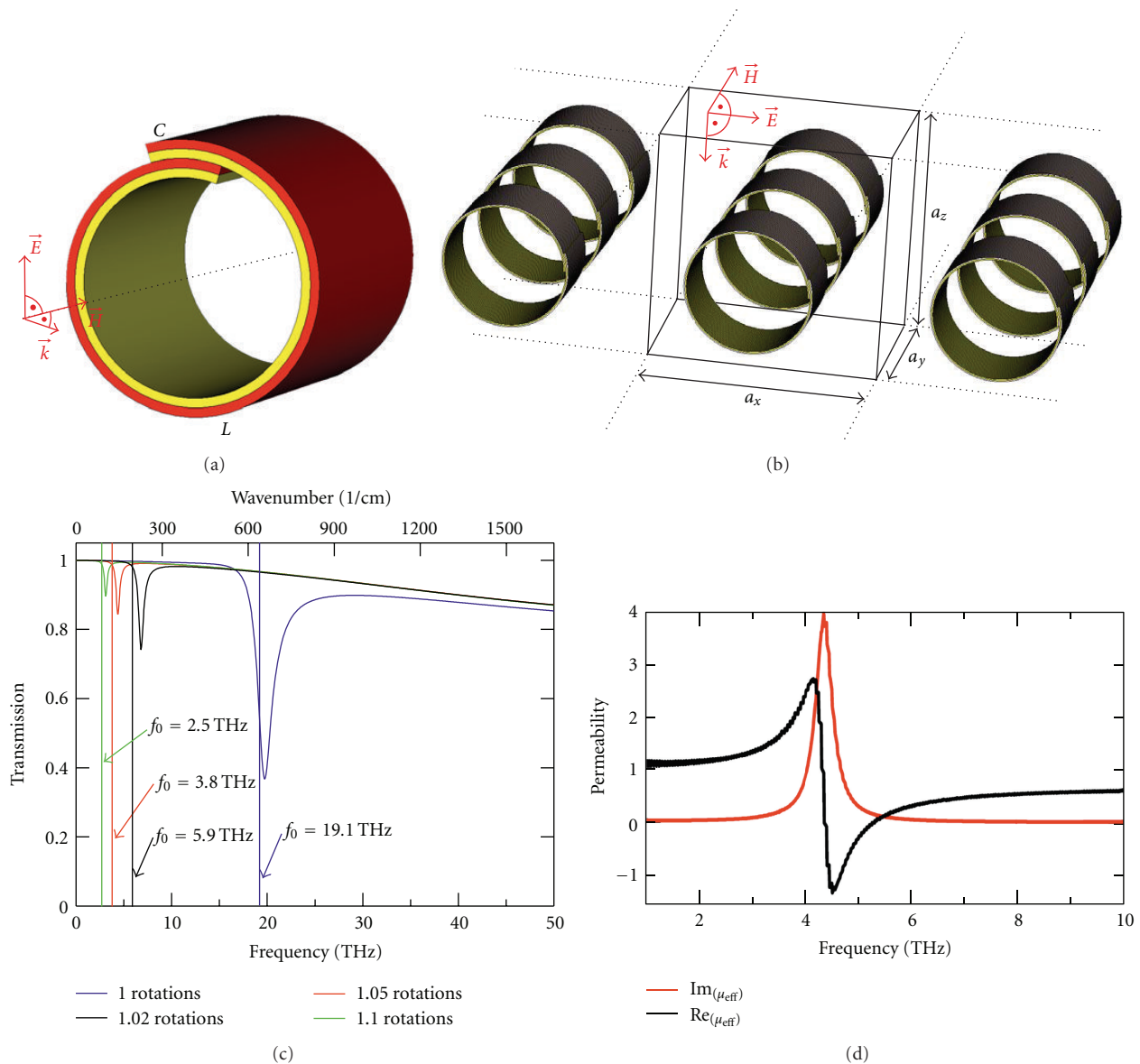


FIGURE 7: (a) Sketch of a microroll consisting of an (In)GaAs (red) and a gold layer (yellow). (b) Simulation setup: black lines indicate the simulation volume with periodic boundary conditions in the x and y direction. A plane wave is incident in z direction with the magnetic field vector pointing along the tube axis; that means in the y direction. (c) Simulated transmission spectra of microroll arrays with varying winding numbers n and the calculated resonance frequencies f_0 . (d) Retrieved complex permeability μ_{eff} of a microroll array for a winding number of $n = 1.05$. Figure reprinted from [33] with slight modifications.

such a three-dimensional fishnet metamaterial. Figure 3(b) depicts the simulated reflection and transmission through the structure. Retrieving the effective refractive index reveals that the real part (n') is negative at the resonance positions in the reflectivity. At the positions where the real part is negative, the effective permeability shows a Lorentzian-shaped resonance (see Figure 3(c)). In Figure 3(d) a prism has been cut into the multilayer stack. As depicted by the black arrows it can be clearly seen that a wave impinging from the left side gets negatively refracted. Calculating the real part

of the refractive index via Snell's law for a frequency of $f = 220$ THz leads to a refractive index of $n' = -1.03$. This is in very good agreement with the refractive index of $n' = -1.07$ calculated from the simulated spectra with the parameter retrieval method by Smith et al. [39]. Apart from the high uniformity and possibility to activate the semiconductor component as discussed above in the fabrication section, our rolled-up fishnet metamaterials have the advantage that they need much thinner functional layers due to the high refractive index of the semiconductor component in

comparison to the commonly discussed fishnet structures based on sequential deposition of metal and materials like MgF_2 or hydrogen silsesquioxane ($n' \approx 1.5$).

5. Optically Active Rolled-Up Metamaterials

The integration of quantum emitters into metamaterials opens up the exciting opportunity to study quantum emitters in tailorable dielectric environments. For hyperbolic metamaterials an enhanced spontaneous emission is expected [40–42]. Furthermore, metamaterials can be optically activated by the integration of quantum emitters, for example, to compensate for the typically very high ohmic losses given by the metallic component of metamaterials or to investigate coupling effects with the metallic components of the metamaterials. A major challenge is the realization of such metamaterials with embedded quantum emitters. Monolayered metamaterials with integrated quantum emitters have been realized as fishnet metamaterials with embedded rhodamine dye molecules [43], slit-ring resonator arrays covered with colloidal quantum dots [44, 45], and slit-ring resonator arrays prepared on top of an InGaAs quantum well heterostructure [46, 47]. Reference [41] is one of the few examples in literature for three-dimensional metamaterials containing quantum emitters. In their work Tumkur et al. sequentially deposited metal layers and polymer layers doped with dye molecules.

As discussed in the fabrication section, three-dimensional rolled-up metamaterials fabricated from semiconductor systems intrinsically offer the possibility to embed high quality quantum structures. In [30] we showed that optically active quantum wells embedded in a hyperlens structure can be used to actively modify the transmission and reduce losses via optical pumping. The investigated structure was based on a semiconductor heterostructure grown by MBE on a GaAs substrate. The functional semiconductor heterostructure consists of a strained $\text{In}_{13}\text{Al}_{20}\text{Ga}_{67}\text{As}$ barrier layer (23 nm), a strained $\text{In}_{16}\text{Ga}_{84}\text{As}$ quantum well (7 nm), and an unstrained $\text{Al}_{23}\text{Ga}_{77}\text{As}$ barrier layer (21 nm). After MBE growth the structure was metalized with an Ag layer (13 nm) and rolled up into a microtube with several rotations. Like the hyperlens structure presented in Section 3, the wall of the rolled-up microtube represents a metamaterial consisting of alternating layers of Ag and semiconductor, but in contrast to the passive hyperlens, it represents an optically active rolled-up metamaterial.

In order to investigate the influence of optical pumping of the embedded quantum well, the transmission enhancement was measured. For that purpose a low-temperature transmission measurement setup operating at liquid helium temperatures was used as sketched in Figure 4(a). In this setup a light emitting fiber tip was inserted into the hollow core of the microtube to illuminate the rolled-up metamaterial from the inside. The light transmitted through the metamaterial was collected by a microscope objective and detected with a single photon counting diode. A pump laser was simultaneously focused onto the outer perimeter of the metamaterial to optically pump the embedded quantum

well. With this setup the transmission enhancement of the metamaterial $\Delta T/T$ was obtained from the transmitted light intensity I_{TPL} under optical excitation of the quantum well, the photoluminescence intensity I_{PL} , when no light is transmitted through the metamaterial, the transmitted intensity I_{T} without pumping of the quantum well, and the dark count intensity I_{D} , as follows: $\Delta T/T = (I_{\text{TPL}} - I_{\text{PL}})/(I_{\text{T}} - I_{\text{D}})$. In Figure 4(b) the transmission enhancement $\Delta T/T$ (squares) of the active rolled-up metamaterial is plotted against the photon energy of the transmitted light. The transmission enhancement has a maximum at a photon energy of $E = 1.36$ eV with a value of $\Delta T/T = 10\%$.

6. Fano Resonance in Optically Active Rolled-Up Plasmonic Metamaterials

After the first observation of optical gain by quantum emitters in a three-dimensional rolled-up metamaterial as discussed above, we in the next step realized rolled-up metamaterials with integrated quantum emitters and plasmonic nanostructures and detected a characteristic Fano resonance caused by the coupling between the quantum emitters and the plasmon polaritons in the plasmonic structures [31]. As a quantum emitter we used a GaAs quantum well (17 nm) embedded between an $\text{In}_{20}\text{Al}_{30}\text{Ga}_{50}\text{As}$ barrier (17 nm) and an $\text{Al}_{20}\text{Ga}_{80}\text{As}$ barrier (17 nm). Before the rolling-up process the upper $\text{Al}_{20}\text{Ga}_{80}\text{As}$ barrier was modulated with a wire profile with a height of $h = 10$ nm, a wire width of $w = 100$ nm and a period of $a = 500$ nm using laser interference lithography and wet chemical etching. Subsequently, a 13 nm thick silver film was deposited onto the modulated surface. Rolling-up this structure along the wire profiles (Figure 5(a)) results in a three-dimensional metamaterial consisting of alternating layers of a quantum well heterostructure and silver wires as sketched in Figure 5(c). Figure 5(b) shows the corresponding scanning electron micrographs of a realized metamaterial. To make the stacked wire structure visible, a hole was cut into the rolled-up metamaterial using focused ion beams. As visible in Figure 5(b) and the corresponding sketch in Figure 5(c) the wires are not perfectly stacked but laterally displaced by Δ due to the finite angle γ between wire direction and rolling direction. For compactly rolled-up systems one obtains $\Delta = \pi(d + 2tN)\tan(\gamma)$, where d is the diameter of the rolled-up metamaterial, t is the single layer thickness, and N is the index of the respective rotation position. We have investigated such stacked lattice structures using finite difference time domain simulations and rigorous coupled wave analysis and found plasmon polariton resonances with a spectral position, which strongly depends on the lattice parameters h , w , a , and Δ . We modeled the embedded quantum well as a Lorentz resonance in the permittivity of the semiconductor component and examined the coupling of the quantum well with the plasmon polaritons. Depending on their spectral overlap and the gain assumed for the quantum well, we predicted characteristic Fano resonances in the pump-induced transmission change. For spectral coincidence and moderate quantum well gain we expect a pumping-induced reduction of transmission and for

very strong quantum well gain we expect a net gain through the metamaterial [32].

In measurements of the pump-induced transmission change $\Delta T/T$ through rolled-up metamaterials as shown in Figure 5 we indeed found characteristic Fano resonances, as depicted in Figure 5(d) [31]. The transmission enhancement $\Delta T/T$ (squares) is plotted against the photon energy of the transmitted light. The measured data can be fitted by applying a Fano resonance model (solid lines) assuming a Fano type resonance interaction between the quantum well resonance and the surface plasmon polariton resonance mediated via the embedded grating. The pumping-induced reduction in the transmission reflects the moderate gain of the GaAs quantum well used in these structures. In the next step it is a very interesting question, if optimization of the coupling and maximization of the quantum well gain might enable net gain through these structures.

7. Rolled-Up Metamaterials for the Terahertz Regime

Instead of using the walls of rolled-up structures as metamaterials for optical frequencies, as discussed above, an alternative approach is to use the entire rolled-up structures as a unit cell of a metamaterial. Prinz and coworkers showed that rolled-up nanostructures also allow the experimental realization of metamaterials with strong chiral properties in the Terahertz regime [34]. An array of (In)GaAs/GaAs/Ti/Au microhelices of 11 μm diameter and 52-53 degree helix angle is shown in Figure 6(a). For the preparation of such helices with well defined helix angle, Prinz and coworkers utilized the strong preferential rolling direction of self-rolling layers in the InGaAs system. A strained mesa, which is aligned to one of the $\langle 100 \rangle$ rolling directions, rolls up into a tube while a strained mesa, which is canted with respect to the rolling direction, rolls up into a helix with helix angle given by the canting angle of the mesa. In polarization resolved transmission measurements Prinz and coworkers found circular dichroism and polarization rotation around 2 THz for the chiral metamaterial shown in Figure 6(a) in agreement with analytical modeling [34]. Figure 6(b) shows a THz metamaterial, which was developed in our group and is based on an array of rolled-up InGaAs/GaAs/Cr microtubes. As schematically illustrated at the bottom right, these structures exhibit slightly more than one rotation and resemble an LC circuit in analogy to the concept of a split ring resonator [3]. In [33] we investigated this type of metamaterial theoretically and found magnetic responses, which can be tuned from a few THz to a few ten THz depending on the number of rotations. Figures 7(a) and 7(b) illustrate the simulation setup. We could show that arrays of gold/(In)GaAs microrolls with slightly more than one winding (see Figure 7(a)) exhibit a negative permeability in the Terahertz regime. Figure 7(c) depicts the transmission spectra of arrays of microrolls with varying winding numbers of $n = 1.00, 1.02, 1.05,$ and 1.10 . Well pronounced resonances are found with frequencies in the Terahertz regime that can be tailored by the winding number. The resonance frequency can be well modeled with

a simple Lorentz-oscillator model. The (In)GaAs in the overlap area is sandwiched between two metal layers that form a capacitance C . The inductivity L of the microroll can be approximated by the inductivity of a ring coil with a single winding. The resonance frequency $f_0 = 1/\sqrt{LC}$ can then be calculated in good agreement with the simulation results (cf. vertical lines in Figure 7(c)). Retrieving the real and imaginary parts of the effective permeability of the array with the parameter retrieval method by Smith et al. [39] reveals that its real part becomes negative near the resonance. This is exemplarily shown for the array with the winding number $n = 1.05$ (Figure 7(d)).

8. Conclusion

In conclusion we reviewed pioneering works for the fabrication and utilization of metamaterials based on self-rolling strained layers including three-dimensional optical metamaterials like broadband rolled-up hyperlenses, rolled-up fishnet metamaterials, and optically active devices containing semiconductor quantum wells as well as THz metamaterials exhibiting circular dichroism and negative permeability. These works demonstrate that the concept of rolled-up metamaterials is a powerful and unique tool to produce three-dimensional metamaterials, optionally with integrated semiconductor quantum emitters, from two-dimensional metamaterial layers. Such robust three-dimensional systems are interesting, for example, for the investigation of the Purcell effect in hyperbolic media [40–42], for gain experiments on stacked plasmonic elements interleaved with quantum emitters [48], or for the realization of polarizers based on stacks of plasmonic structures [49].

Acknowledgments

The authors thank Markus Bröll and Detlef Heitmann for many fruitful discussions on rolled-up metamaterials. They also thank David Sonnenberg, Andrea Stemmann, Christian Heyn, and Wolfgang Hansen for the growth of the molecular beam epitaxy samples and Yulia Stark, Daniel Stickler, and Hans-Peter Oepen for focused ion beam preparation. The authors acknowledge financial support by the Deutsche Forschungsgemeinschaft via SFB508, SFB668, GK1286 and financial support by the city of Hamburg via LExI “Nanospintronics”.

References

- [1] H. O. Moser and C. Rockstuhl, “3D THz metamaterials from micro/nanomanufacturing,” *Laser and Photonics Reviews*, vol. 6, no. 2, pp. 219–244, 2012.
- [2] C. M. Soukoulis and M. Wegener, “Past achievements and future challenges in the development of three-dimensional photonic metamaterials,” *Nature Photonics*, vol. 5, article 523, 2011.
- [3] J. B. Pendry, A. J. Holden, D. J. Robbins, and W. J. Stewart, “Magnetism from conductors and enhanced nonlinear phenomena,” *IEEE Transactions on Microwave Theory and Techniques*, vol. 47, no. 11, pp. 2075–2084, 1999.

- [4] R. A. Shelby, D. R. Smith, and S. Schultz, "Experimental verification of a negative index of refraction," *Science*, vol. 292, no. 5514, pp. 77–79, 2001.
- [5] A. A. Houck, J. B. Brock, and I. L. Chuang, "Experimental observations of a left-handed material that obeys Snell's law," *Physical Review Letters*, vol. 90, no. 13, Article ID 137401, 4 pages, 2003.
- [6] D. Schurig, J. J. Mock, B. J. Justice et al., "Metamaterial electromagnetic cloak at microwave frequencies," *Science*, vol. 314, no. 5801, pp. 977–980, 2006.
- [7] N. Liu, H. Guo, L. Fu, S. Kaiser, H. Schweizer, and H. Giessen, "Three-dimensional photonic metamaterials at optical frequencies," *Nature Materials*, vol. 7, no. 1, pp. 31–37, 2008.
- [8] J. Valentine, S. Zhang, T. Zentgraf et al., "Three-dimensional optical metamaterial with a negative refractive index," *Nature*, vol. 455, no. 7211, pp. 376–379, 2008.
- [9] J. Rho, Z. Ye, Y. Xiong et al., "Spherical hyperlens for two-dimensional sub-diffractive imaging at visible frequencies," *Nature Communications*, vol. 1, no. 9, article 143, 2010.
- [10] Z. Liu, H. Lee, Y. Xiong, C. Sun, and X. Zhang, "Far-field optical hyperlens magnifying sub-diffraction-limited objects," *Science*, vol. 315, no. 5819, p. 1686, 2007.
- [11] J. K. Gansel, M. Thiel, M. S. Rill et al., "Gold helix photonic metamaterial as broadband circular polarizer," *Science*, vol. 325, no. 5947, pp. 1513–1515, 2009.
- [12] J. Yao, Z. Liu, Y. Liu et al., "Optical negative refraction in bulk metamaterials of nanowires," *Science*, vol. 321, no. 5891, p. 930, 2008.
- [13] N. Gibbons, J. J. Baumberg, C. L. Bower, M. Kolle, and U. Steiner, "Scalable cylindrical metallodielectric metamaterials," *Advanced Materials*, vol. 21, no. 38-39, pp. 3933–3936, 2009.
- [14] V. Ya Prinz, V. A. Seleznev, and A. K. Gutakovskiy, "Self-formed InGaAs/GaAs Nanotubes: Concept, Fabrication, Properties," in *Proceedings of the 25th International Conference on the Physics of Semiconductors*, Jerusalem, Israel, 1998.
- [15] V. Y. Prinz, V. A. Seleznev, A. K. Gutakovskiy et al., "Free-standing and overgrown InGaAs/GaAs nanotubes, nano-helices and their arrays," *Physica E*, vol. 6, no. 1, pp. 828–831, 2000.
- [16] S. V. Golod, V. Y. Prinz, V. I. Mashanov, and A. K. Gutakovskiy, "Fabrication of conducting GeSi/Si micro- and nanotubes and helical microcoils," *Semiconductor Science and Technology*, vol. 16, no. 3, pp. 181–185, 2001.
- [17] O. Schumacher, S. Mendach, H. Welsch, A. Schramm, C. Heyn, and W. Hansen, "Lithographically defined metal-semiconductor-hybrid nanoscrolls," *Applied Physics Letters*, vol. 86, no. 14, Article ID 143109, 3 pages, 2005.
- [18] C. Deneke, W. Sigle, U. Eigenthaler, P. A. Van Aken, G. Schütz, and O. G. Schmidt, "Interfaces in semiconductor/metal radial superlattices," *Applied Physics Letters*, vol. 90, no. 26, Article ID 263107, 3 pages, 2007.
- [19] Y. Mei, G. Huang, A. A. Solov'ev et al., "Versatile approach for integrative and functionalized tubes by strain engineering of nanomembranes on polymers," *Advanced Materials*, vol. 20, no. 21, pp. 4085–4090, 2008.
- [20] F. Balhorn, S. Mansfeld, A. Krohn et al., "Spin-wave interference in three-dimensional rolled-up ferromagnetic microtubes," *Physical Review Letters*, vol. 104, no. 3, Article ID 037205, 4 pages, 2010.
- [21] F. M. Huang, J. K. Sinha, N. Gibbons, P. N. Bartlett, and J. J. Baumberg, "Direct assembly of three-dimensional mesh plasmonic rolls," *Applied Physics Letters*, vol. 100, no. 19, Article ID 193107, 4 pages, 2012.
- [22] O. G. Schmidt and K. Eberl, "Thin solid films roll up into nanotubes," *Nature*, vol. 410, article 168, 2001.
- [23] E. J. Smith, Z. Liu, Y. Mei, and O. G. Schmidt, "Combined surface plasmon and classical waveguiding through metamaterial fiber design," *Nano Letters*, vol. 10, no. 1, pp. 1–5, 2010.
- [24] E. J. Smith, Z. Liu, Y. F. Mei, and O. G. Schmidt, "System investigation of a rolled-up metamaterial optical hyperlens structure," *Applied Physics Letters*, vol. 95, no. 8, Article ID 083104, 3 pages, 2009.
- [25] E. J. Smith, Z. Liu, Y. F. Mei, and O. G. Schmidt, "Erratum: 'System investigation of a rolled-up metamaterial optical hyperlens structure' [*Appl. Phys. Lett.* 95, 083104 (2009)]," *Applied Physics Letters*, vol. 96, no. 1, Article ID 019902, 2 pages, 2010.
- [26] S. Schwaiger, M. Bröll, A. Krohn et al., "Rolled-up three-dimensional metamaterials with a tunable plasma frequency in the visible regime," *Physical Review Letters*, vol. 102, no. 16, Article ID 163903, 4 pages, 2009.
- [27] S. Schwaiger, A. Rottler, M. Bröll et al., "Broadband operation of rolled-up hyperlenses," *Physical Review B*, vol. 85, no. 23, Article ID 235309, 9 pages, 2012.
- [28] J. Kerbst, S. Schwaiger, A. Rottler et al., "Enhanced transmission in rolled-up hyperlenses utilizing Fabry-Pérot resonances," *Applied Physics Letters*, vol. 99, no. 19, Article ID 191905, 3 pages, 2011.
- [29] A. Rottler, M. Harland, M. Bröll et al., "Rolled-up nanotechnology for the fabrication of three-dimensional fishnet-type GaAs-metal metamaterials with negative refractive index at near-infrared frequencies," *Applied Physics Letters*, vol. 100, no. 15, Article ID 151104, 4 pages, 2012.
- [30] S. Schwaiger, M. Klingbeil, J. Kerbst et al., "Gain in three-dimensional metamaterials utilizing semiconductor quantum structures," *Physical Review B*, vol. 84, no. 15, Article ID 155325, 5 pages, 2011.
- [31] S. Schwaiger, A. Koitmäe, L. S. Fohrmann et al., "Fano resonances in optically active rolled-up three dimensional metamaterials," unpublished.
- [32] A. Rottler, S. Schwaiger, A. Koitmäe, D. Heitmann, and S. Mendach, "Transmission enhancement in three-dimensional rolled-up plasmonic metamaterials containing optically active quantum wells," *Journal of the Optical Society of America B*, vol. 28, no. 10, pp. 2402–2407, 2011.
- [33] A. Rottler, M. Bröll, N. Gerken, D. Heitmann, and S. Mendach, "Terahertz metamaterials based on arrays of rolled-up gold/(In)GaAs tubes," *Optics Letters*, vol. 36, no. 24, pp. 4797–4799, 2011.
- [34] I. V. Semchenko, S. A. Khakhomov, E. V. Naumova, V. Y. Prinz, S. V. Golod, and V. V. Kubarev, "Study of the properties of artificial anisotropic structures with high chirality," *Crystallography Reports*, vol. 56, no. 3, pp. 366–373, 2011.
- [35] B. Wood, J. B. Pendry, and D. P. Tsai, "Directed subwavelength imaging using a layered metal-dielectric system," *Physical Review B*, vol. 74, no. 11, Article ID 115116, 8 pages, 2006.
- [36] S. A. Ramakrishna and J. B. Pendry, "Removal of absorption and increase in resolution in a near-field lens via optical gain," *Physical Review B*, vol. 67, no. 20, Article ID 201101, 4 pages, 2003.
- [37] D. R. Smith, D. Schurig, M. Rosenbluth, S. Schultz, S. A. Ramakrishna, and J. B. Pendry, "Limitations on subdiffraction imaging with a negative refractive index slab," *Applied Physics Letters*, vol. 82, no. 10, pp. 1506–1508, 2003.

- [38] Z. Jacob, L. V. Alekseyev, and E. Narimanov, "Optical hyperlens: far-field imaging beyond the diffraction limit," *Optics Express*, vol. 14, no. 18, pp. 8247–8256, 2006.
- [39] D. R. Smith, D. C. Vier, T. Koschny, and C. M. Soukoulis, "Electromagnetic parameter retrieval from inhomogeneous metamaterials," *Physical Review E*, vol. 71, no. 3, Article ID 036617, 11 pages, 2005.
- [40] M. A. Noginov, H. Li, Y. A. Barnakov et al., "Controlling spontaneous emission with metamaterials," *Optics Letters*, vol. 35, no. 11, pp. 1863–1865, 2010.
- [41] T. Tumkur, G. Zhu, P. Black, Y. A. Barnakov, C. E. Bonner, and M. A. Noginov, "Control of spontaneous emission in a volume of functionalized hyperbolic metamaterial," *Applied Physics Letters*, vol. 99, no. 15, Article ID 151115, 3 pages, 2011.
- [42] H. N. S. Krishnamoorthy, Z. Jacob, E. Narimanov, I. Kretzschmar, and V. M. Menon, "Topological transitions in metamaterials," *Science*, vol. 336, no. 6078, pp. 205–209, 2012.
- [43] S. Xiao, V. P. Drachev, A. V. Kildishev et al., "Loss-free and active optical negative-index metamaterials," *Nature*, vol. 466, no. 7307, pp. 735–738, 2010.
- [44] E. Plum, V. A. Fedotov, P. Kuo, D. P. Tsai, and N. I. Zheludev, "Towards the lasing spaser: controlling metamaterial optical response with semiconductor quantum dots," *Optics Express*, vol. 17, no. 10, pp. 8548–8551, 2009.
- [45] K. Tanaka, E. Plum, J. Y. Ou, T. Uchino, and N. I. Zheludev, "Multifold enhancement of quantum dot luminescence in plasmonic metamaterials," *Physical Review Letters*, vol. 105, no. 22, Article ID 227403, 4 pages, 2010.
- [46] N. Meinzer, M. Ruther, S. Linden et al., "Arrays of Ag splitting resonators coupled to InGaAs single-quantum-well gain," *Optics Express*, vol. 18, no. 23, pp. 24140–24151, 2010.
- [47] N. Meinzer, M. König, M. Ruther et al., "Distance-dependence of the coupling between split-ring resonators and single-quantum-well gain," *Applied Physics Letters*, vol. 99, no. 11, Article ID 111104, 3 pages, 2011.
- [48] D. J. Bergman and M. I. Stockman, "Surface plasmon amplification by stimulated emission of radiation: quantum generation of coherent surface plasmons in nanosystems," *Physical Review Letters*, vol. 90, no. 2, Article ID 027402, 4 pages, 2003.
- [49] Y. Zhao, M. A. Belkin, and A. Alù, "Twisted optical metamaterials for planarized ultrathin broadband circular polarizers," *Nature Communications*, vol. 3, article 870, 2012.



Hindawi

Submit your manuscripts at
<http://www.hindawi.com>

